Analysis of Cake Growth in Cake Filtration: Effect of Fine Particle Retention

Chi Tien, Renbi Bai, and B. V. Ramarao
Dept. of Chemical Engineering, National University of Singapore, Singapore 119260

Equations were derived that describe the dynamics of cake growth in cake filtration, and methods for their solutions were developed. In deriving the equations, the moving boundary nature of the cake formation process and the effect of fine particle retention were considered. It was shown that fine particle retention may contribute significantly to the decrease of cake permeability and thus alters the performance of cake filtration even if the amount of fine particles involved is small. Through numerical examples, it was also demonstrated that fine particle retention in filter cakes may cause serious errors in determining the constitutive relationships from filter test data.

Introduction

Cake filtration has been practiced for a long time in engineering. In cake filtration, a slurry to be treated is passed through a medium with openings smaller than the diameters of most of the particles present in the slurry. Separation is accomplished by retaining particles at the surface of the medium, leading to the formation of a cake. The cake thickness increases with time. Furthermore, the cake structure may undergo changes as a result of cake compression caused by the drag forces acting on the retained particles by the slurry flow. This change in cake structure, in turn, may affect the filtration performance.

Analysis of cake filtration began with the classical work of Ruth et al. (1933) more than half a century ago. Since that time, a body of literature on cake filtration has been developed (for a summary, see Shirato et al., 1987). To account for cake inhomogeneity, the use of average permeability (or specific resistance) has been adopted and empirical constitutive equations relating the cake porosity and permeability with the applied compressive stress have been proposed (see, e.g., Tiller and Yeh, 1986). An important fact to be recognized in cake filtration is that the solids phase is also under movement during the formation and development of the cake. Tiller and Cooper (1960) derived a relation based on the porosity change and the flow velocity variation. As shown by Shirato et al. (1969) and by Tiller and Shirato (1964), the variation of internal porosity and flow rate within the cakes can sometimes be quite significant. Based on their studies, Tiller and Shirato (1964) proposed to modify the relation between filtrate volume and time by a correction factor.

More rigorous analyses of filtration start from the continuity equations for the solid and liquid phases within the cake. It is possible to derive a nonlinear partial differential equation relating the cake solidosity with solid pressure (see, e.g., Wakeman, 1978). A derivation of the equations of cake filtration from multiphase flow models as well as the validity of various approximate theories have been provided by Willis et al. (1991). A continuum analysis of the cake filtration problem and comparisons with experimental data on filtration of solka-flocs were given by Chase (1989). More recently, Stamatakis and Tien (1991) presented a numerical solution of cake growth taking into account both solid and liquid flow, variations of cake porosity and permeability, and the moving boundary nature of the problem.

In actual filtration, the sizes of the particles present in a suspension often cover a wide range. While the majority of the particles are retained to form a cake, a small amount of finer ones may penetrate into the cake. The permeability of a cake therefore depends upon the extent of the compression to which it is subject, as well as the amount of fines retained within the cake. Conventional cake theories, in general, have failed to consider the effect of fine particle retention.

In predicting cake filtration performance, ignoring the effect of fine particle retention may lead to an overestimation of the compression effect on cake permeability since a small amount of fine retention may significantly clog a cake. On the other hand, in determining constitutive relationships from experimental filter data, unless the effect of fine particle re-

B. V. Ramaro is on leave from the Faculty of Paper Science and Engineering, SUNY, ESF, Syracuse, NY 13210.

tention is properly accounted for, the resulting relationship could be in serious error.

This work presents a rigorous analysis of cake filtration which considers the effect of fine particle retention within the cake formed. A numerical algorithm was developed for the solution of the governing equations. As part of the work, an example is also presented to illustrate the errors in constitutive relationships if experimental data were interpreted without considering the effect of fine particle retention.

Analysis

Statement of problem

The problem may be stated as follows: A solid-liquid suspension is passed through a septum (or a medium). The majority of particles of the suspension are too large to pass through the medium. Consequently, they become retained at the medium surface to form a cake. This cake grows in thickness and is compressed. It also functions as a granular filter and retains some of the finer particles as they flow through the cake. Both compression and fine particle retention within the cake tend to decrease the cake permeability. The analysis is aimed at examining this problem in a rigorous way.

Assumptions

The following assumptions are used in formulating the analysis:

(a) The suspended particles will be considered to be of two types: Type 1 with diameter d_{p1} which, because of its size, is retained completely at the cake-slurry interface (or at the septum surface initially), and Type 2 with diameter d_{p2}, which penetrates into the cake but may be retained within the cake. The type 1 particle concentration is much greater than that of particles of type 2. Based on particle deposition considerations (Tien, 1989), $d_{p2}/d_{p1} < 10^{-1}$.

(b) The formation of a cake from suspension is characterized by a threshold value of the volume fraction of particles. In other words, at the slurry-cake interface, there is a discontinuity.

(c) The coordinate system used is shown in Figure 1.

(d) The slurry flow is unidirectional, with particle and liquid velocities being the same.

(e) There is no particle retention within the septum.

The various relevant quantities used in the analysis are: The particle concentrations of the suspension are represented as volume of particles per unit volume of suspension. c, c_1, and c_2 denote respectively the total particle, type 1 particle and type 2 particle concentrations. By definition

$$c = c_1 + c_2 \tag{1}$$

Alternatively, these particle concentrations may be expressed as volume of particles per unit volume of the suspending liquid, denoted as n, n_1, and n_2 and

$$n = n_1 + n_2 \tag{2}$$

The relationships between the ns and cs are: (noting $n_2 \ll n_1 < 1$)

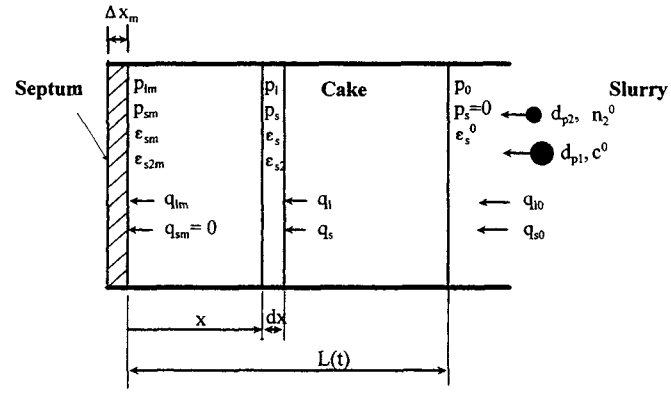

Figure 1. Cake filtration and the coordinate system used in the analysis.

$$c_1 = n_1/(1 + n_1 + n_2) \approx n_1/(1 + n_1) \tag{3}$$

$$c_2 = n_2/(1 + n_1 + n_2) \approx n_2/(1 + n_1) \tag{4}$$

For suspensions flowing through the cake, since particles of type 1 are completely retained at the cake-slurry interface, one has

$$c_1 = n_1 = 0 \tag{5}$$

and

$$c_2 \approx n_2 \tag{6}$$

To characterize the cake structure, the cake porosity ϵ is defined as the volume of the void space per unit volume of cake. The solidosity ϵ_s is defined as the fraction of solids per unit volume of cake. ϵ_s is given as

$$\epsilon_s = 1 - \epsilon \tag{7}$$

Since particles are of two types, let ϵ_{s1} and ϵ_{s2} denote the volume fractions of particles of type 1 and type 2 respectively. ϵ_{s1}, ϵ_{s2} and ϵ_s are related by the equation

$$\epsilon_s = \epsilon_{s1} + \epsilon_{s2} \tag{8}$$

The composition of the cake may be characterized by any two of the three quantities, ϵ_s, ϵ and ϵ_{s2}.

For a compressible cake under formation, both liquid and solid move toward the septum. q_l and q_s denote the liquid and solid superficial velocities. q_s is, in general, a small quantity. However, it is a critical factor in determining the extent of cake compression.

The pressure of the liquid phase is denoted by p. The compressible stress of the solid phase due to the cumulative drag forces exerted on the cake particles is p_s. If the inertial effect is negligible, one has

$$p + p_s = p_0 \tag{9}$$

where p_0 is the pressure at the cake-slurry interface. The derivation of Eq. 9 can be found in Tiller and Crump (1985).

In making the analysis, the following principles are used:

(a) Conservation equations
(b) First-order rate expression for fine particle retention
(c) Darcy's law for the relative motion of the fluid within the cake
(d) Constitutive relations between ϵ_s (or k, the local permeability) with p_s
(e) A power-law expression between the change in k and the extent of type 2 particle retention ϵ_{s2}.

The basic equations describing cake growth are (in the equations given below, it is assumed that the suspension velocity and the velocity of suspending liquid through the cake are essentially the same since the concentration of the type 2 particles c_2 is small).

Conservation Equations

(a) The conservation equation of liquid is given as

$$\frac{\partial q_l}{\partial x} = \frac{\partial \epsilon_s}{\partial t} \tag{10}$$

(b) The conservation equation of solid is

$$-\frac{\partial}{\partial x}(q_l n_2) - \frac{\partial q_s}{\partial x} = \frac{\partial \epsilon_s}{\partial t} + \frac{\partial}{\partial t}[(1-\epsilon_s)n_2] \tag{11}$$

(c) The conservation equation of particles of type 2 is

$$-\frac{\partial}{\partial x}(q_l n_2) - \frac{\partial}{\partial x}\left(q_s \frac{\epsilon_{s2}}{\epsilon_s}\right) = \frac{\partial \epsilon_{s2}}{\partial t} + \frac{\partial}{\partial t}[(1-\epsilon_s)n_2] \tag{12}$$

(d) The conservation equation of particles of type 2 in the solid phase is (for cases there are more than two types of particles present in the slurry, and $d_{p1} \gg d_{p2}, d_{p3}, \ldots\ldots$, additional equations similar to Eq. 13, each with its own rate of deposition N_i $i = 2, 3, \ldots\ldots$):

$$-\frac{\partial}{\partial x}\left(q_s \frac{\epsilon_{s2}}{\epsilon_s}\right) + N = \frac{\partial \epsilon_{s2}}{\partial t} \tag{13}$$

where N is the rate of deposition of particles of type 2 per unit volume of cake.

By combining Eq. 12 with Eq. 13, one has

$$-\frac{\partial}{\partial x}(q_l n_2) - N = \frac{\partial}{\partial t}[(1-\epsilon_s)n_2] \tag{14}$$

Similarly, one may eliminate $\partial \epsilon_s/\partial t$ from Eqs. 10 and 11 to give

$$\frac{\partial}{\partial x}(q_l n_2) + \frac{\partial q_l}{\partial x} + \frac{\partial q_s}{\partial x} = -\frac{\partial}{\partial t}[(1-\epsilon_s)n_2] \tag{15}$$

By eliminating $\partial/\partial t\,[(1-\epsilon_s)n_2]$ and $\partial/\partial x\,(q_l n_2)$ from Eqs. 14 and 15, one has

$$\frac{\partial}{\partial x}(q_l + q_s) = N \tag{16}$$

which, upon integration, gives

$$(q_l + q_s) - (q_l + q_s)_{x=0} = \int_0^x N dx \tag{17a}$$

At the medium surface, $q_s = 0$ and q_l is the permeation velocity of filtrate through the septum (or filtrate velocity), q_{lm}. Integration of Eq. 16 yields

$$(q_l + q_s) = q_{lm} + \int_0^x N dx \tag{17b}$$

Expression of Fine Particle Retention Rate. In deep-bed filtration, the rate of retention is proportional to the product of the suspension concentration and the suspension superficial velocity with the proportionality constant λ known as the filter coefficient (Tien, 1989). For a cake under formation, since both the liquid and the solid phases move simultaneously, the velocity term is now replaced by the relative liquid velocity (with respect to solid) or

$$\left[\frac{q_l}{1-\epsilon_s} - \frac{q_s}{\epsilon_s}\right]\cdot(1-\epsilon_s)$$

The expression within the parenthesis is the liquid velocity relative to that of the solid. Multiplying the quantity by $(1-\epsilon_s)$ converts the velocity to the superficial velocity. N can therefore be expressed as

$$N = \left|q_l - q_s \frac{1-\epsilon_s}{\epsilon_s}\right| \lambda n_2 \tag{18}$$

where $|\ \ |$ represents the absolute value.

Darcy's Law. Darcy's law may be used to relate the pressure gradient to the liquid and solid superficial velocities q_l and q_s. The expression is

$$\left(\frac{q_l}{1-\epsilon_s} - \frac{q_s}{\epsilon_s}\right) = -\frac{k}{(1-\epsilon_s)\mu}\frac{\partial p}{\partial x} \tag{19a}$$

or

$$\epsilon_s q_l - (1-\epsilon_s)q_s = -\epsilon_s\left(\frac{k}{\mu}\frac{\partial p}{\partial x}\right) \tag{19b}$$

Upon rearrangement, one has

$$q_l - (1-\epsilon_s)(q_l + q_s) = -\epsilon_s\left(\frac{k}{\mu}\frac{\partial p}{\partial x}\right) \tag{20}$$

Substituting Eq. 17b into Eq. 20, one has

$$q_l = -\epsilon_s\left(\frac{k}{\mu}\frac{\partial p}{\partial x}\right) + (1-\epsilon_s)q_{lm} + (1-\epsilon_s)\int_0^x N dx \tag{21}$$

The expression of q_s can now be derived. First, from Eq. 17, one has

$$q_s = -q_l + q_{lm} + \int_0^x N dx \tag{22}$$

Substituting Eq. 21 into Eq. 22, one has

$$q_s = \epsilon_s\left(\frac{k}{\mu}\frac{\partial p}{\partial x}\right) + \epsilon_s q_{lm} + \epsilon_s\int_0^x N dx \tag{23}$$

The governing equations can now be obtained. First substituting Eq. 21 (expression of q_l) into Eq. 10, one has

$$\frac{\partial \epsilon_s}{\partial t} = -\frac{\partial}{\partial x}\left[\epsilon_s\frac{k}{\mu}\frac{\partial p}{\partial x}\right] - \left[q_{lm} + \int_0^x N dx\right]\frac{\partial \epsilon_s}{\partial x} + (1-\epsilon_s)N \tag{24}$$

Next substituting Eq. 18 (expression of N) into Eq. 13 yields

$$\frac{\partial \epsilon_{s2}}{\partial t} = -\frac{\partial}{\partial x}\left(q_s\frac{\epsilon_{s2}}{\epsilon_s}\right) + \left|q_l - \frac{1-\epsilon_s}{\epsilon_s}q_s\right|\lambda n_2 \tag{25}$$

As discussed before, q_{lm} is the value of q_l at $x = 0$. By definition, q_{lm} may be written as

$$q_{lm} = -\left(\frac{k}{\mu}\frac{\partial p}{\partial x}\right)_0 = -\frac{k_m}{\Delta x_m \mu}(p|_{x=0}) = -\frac{k_m}{\Delta x_m \mu}(p_0 - p_s|_{x=0}) \tag{26}$$

where Δx_m is the medium's thickness and k_m is the medium permeability. μ is the viscosity of the liquid, and k is the cake permeability. With q_l and q_{lm} given, Eqs. 24, 25 and 12 have ϵ_s, ϵ_{s2} and n_2 as their dependable variables since p (or p_s) or k can be expressed in terms of ϵ_s and ϵ_{s2} through the constitutive equations and the relationship between the decrease of k and the extent of media clogging. This will be discussed as follows.

Constitutive Relationships. The compressible behavior of a filter cake may be described as

$$\epsilon_s = \epsilon_s^0\left(1 + \frac{p_s}{p_A}\right)^{\beta} \tag{27}$$

where ϵ_s^0 is the cake solidosity at the zero compressive stress state and p_A is an empirical constant. For cake permeability, one must include both the compression effect and the presence of deposited fine particles. The combination of these two effects is (Shirato et al., 1987; Tien, 1989)

$$k = k^0\left(1 + \frac{p_s}{p_A}\right)^{-\delta}(1 + \alpha_1\epsilon_{s2}^{\alpha_2})^{-1} \tag{28}$$

or

$$\left[\frac{k}{k^0}(1 + \alpha_1\epsilon_{s2}^{\alpha_2})\right]^{-1/\delta} = 1 + \frac{p_s}{p_A} \tag{29}$$

where δ, α_1, α_2 are empirical constants.

Similarly, one may write

$$\left[\frac{\epsilon_s}{\epsilon_s^0}\right]^{1/\beta} = 1 + \frac{p_s}{p_A} \tag{30}$$

Combining the above two expressions, one has

$$\frac{k}{k^0}(1 + \alpha_1\epsilon_{s2}^{\alpha_2}) = \left(\frac{\epsilon_s}{\epsilon_s^0}\right)^{-\delta/\beta} \tag{31}$$

and

$$p_s = p_A\left[\left(\frac{\epsilon_s}{\epsilon_s^0}\right)^{1/\beta} - 1\right] \tag{32}$$

In summary, the governing equations are therefore Eqs. 24, 25, 14, 23, 21, 26, 31, 32 and 9.

Boundary Conditions. The boundary conditions are

$$x = L, \qquad p_s = 0, \qquad \epsilon_s = \epsilon_s^0 \tag{33}$$

$$x = 0, \qquad \frac{k_m}{\Delta x_m \mu}(p_0 - p_s) = \left(\frac{k}{\mu}\frac{\partial p_s}{\partial x}\right)_{x=0} \tag{34}$$

Slurry-cake interface conditions

The condition describing the cake growth at the interface may be derived as follows: The particle volume fractions on either side of the interface $x = L^-$ (cake) and $x = L^+$ (slurry) are ϵ_s^0 and c^0. Further, all solids in the slurry may be considered to be of particles of type 1 (since $n_1^0 \gg n_2^0$) in cake formation. Over a time interval δt the cake thickness is increased by δL. Mass balances of liquid and solids yield

$$(q_{li} - q_{l0})\delta t = \delta L[(1-\epsilon_s^0) - (1-c^0)] \quad \text{liquid balance} \tag{35a}$$

$$(q_{si} - q_{s0})\delta t = \delta L[\epsilon_s^0 - c^0] \quad \text{solid balance} \tag{35b}$$

where q_{li} and q_{l0} denote, respectively, the liquid superficial velocity on the cake and slurry side at the interface. q_{si} and q_{s0} are the solid superficial velocity similarly defined.

By adding Eq. 35a to Eq. 35b, one has

$$(q_{li} + q_{si}) = (q_{l0} + q_{s0}) \tag{36}$$

On account of Eq. 17b, one has

$$q_{li} + q_{si} = q_{lo} + q_{so} = q_{lm} + \int_0^L N dx \tag{37}$$

From Eq. 35a, one may obtain

$$\frac{dL}{dt} = \frac{q_{li} - q_{lo}}{c^0 - \epsilon_s^0} \tag{38}$$

By applying Darcy's law, namely Eq. 19a at the septum surface ($x = 0$) and at the cake-slurry interface ($x = L$), one has

$$q_{lm} = -\left(\frac{k}{\mu}\frac{\partial p}{\partial x}\right)_0 \tag{39}$$

$$q_{li} = \frac{1-\epsilon_s^0}{\epsilon_s^0} q_{si} - \left(\frac{k}{\mu}\frac{\partial p}{\partial x}\right)_{L^-} \tag{40}$$

q_{si} therefore can be expressed as

$$q_{si} = \frac{\epsilon_s^0}{1-\epsilon_s^0}\left[q_{li} + \left(\frac{k}{\mu}\frac{\partial p}{\partial x}\right)_{L^-}\right] \tag{41}$$

Substituting Eqs. 39 and 41 into 37, one has

$$q_{li} + \frac{\epsilon_s^0}{1-\epsilon_s^0}\left[q_{li} + \left(\frac{k}{\mu}\frac{\partial p}{\partial x}\right)_{L^-}\right] = -\left(\frac{k}{\mu}\frac{\partial p}{\partial x}\right)_0 + \int_0^L N dx \tag{42a}$$

Solving for q_{li}, one has

$$q_{li} = -\epsilon_s^0\left(\frac{k}{\mu}\frac{\partial p}{\partial x}\right)_{L^-} - (1-\epsilon_s^0)\left(\frac{k}{\mu}\frac{\partial p}{\partial x}\right)_0 + (1-\epsilon_s^0)\int_0^L N dx \tag{42b}$$

In the slurry phase, particles and liquids move at the same velocity, one has

$$\frac{q_{so}}{q_{lo}} = \frac{c^0}{1-c^0} \tag{43}$$

or

$$q_{so} = q_{lo}\frac{c^0}{1-c^0} \tag{44}$$

Substituting the above expression into Eq. 37 and solving for q_{l0}, one has

$$q_{l0} = -(1-c^0)\left(\frac{k}{\mu}\frac{\partial p}{\partial x}\right)_0 + (1-c^0)\int_0^L N dx \tag{45}$$

To obtain $q_{li} - q_{l0}$, subtract Eq. 45 from Eq. 42b,

$$q_{li} - q_{lo} = -\epsilon_s^0\left(\frac{k}{\mu}\frac{\partial p}{\partial x}\right)_{L^-} + (\epsilon_s^0 - c^0)\left(\frac{k}{\mu}\frac{\partial p}{\partial x}\right)_0 - (\epsilon_s^0 - c^0)\int_0^L N dx \tag{46}$$

Substituting the above expression into Eq. 38, one has

$$\frac{dL}{dt} = \frac{\epsilon_s^0}{\epsilon_s^0 - c^0}\left(\frac{k}{\mu}\frac{\partial p}{\partial x}\right)_{L^-} - \left(\frac{k}{\mu}\frac{\partial p}{\partial x}\right)_0 + \int_0^L N dx \tag{47}$$

The initial condition is

$$t = 0, \qquad L = 0 \tag{48}$$

Numerical Solution

The system of Eqs. 24, 25, 14, 21, 23 and 26 with boundary conditions of Eqs. 33 and 34 over the spatial domain of $0 < x < L(t)$ together with the constitutive relationships (Eqs. 31 and 32) and the cake growth expressions of Eqs. 47 and 48 describe cake formation and growth. The dependent variables are p_s, p_0, ϵ_s, ϵ_{s2}, n_2 which are functions of x and t, and q_{lm} which is a function of time (for the constant pressure case).

A subroutine D03PCF from NAG Fortran Library (Mark 16) was used to solve the system of equations. D03PCF Subroutine was developed for systems of partial differential equations (PDEs) of the following form

$$\sum_{j=1}^{M} P_{ij}\frac{\partial U_j}{\partial t} + Q_i = \frac{\partial R_i}{\partial x} \quad (i = 1, 2, \ldots, M) \tag{49}$$

where x and t are the spatial and time variables. P_{ij}, Q_i and R_i are functions of x, t, U and U_x where U is the set of solution values of U_j, and the vector U_x is its partial derivative with respect to x. Furthermore, P_{ij}, Q_i and R_i must not depend on $\partial U/\partial t$. M is the number of PDEs. This subroutine uses the method of lines to reduce the PDEs to a system of ordinary differential equations. The boundary conditions required by D03PCF are of the form

$$\beta_i(x,t)R_i(x,t,U,U_x) = \gamma_i(x,t,U,U_x) \quad (i = 1, 2, \ldots, M) \tag{50}$$

The integration is carried out from t_0 to t_{out} over the spatial interval $a \le x \le b$.

Transformation of the governing equations

In order to use D03PCF, it is necessary to transform Eqs. 24, 25 and 14 into the form of Eq. 49. From Eqs. 31 and 32, one has

$$\frac{k}{\mu}\frac{\partial p_s}{\partial x} = \frac{k^0 p_A}{\mu\beta}\left(\frac{\epsilon_s}{\epsilon_s^0}\right)^{(1-\delta)/\beta} \epsilon_s^{-1}(1+\alpha_1\epsilon_{s2}^{\alpha_2})^{-1}\frac{\partial \epsilon_s}{\partial x} \tag{51}$$

To immobilize the moving boundary (i.e., the cake-slurry interface), a new independent variable η is introduced to replace x. η is defined as

$$\eta = x/L \tag{52}$$

The final forms of equations used in the numerical solution are

$$\frac{\partial \epsilon_s}{\partial t} - \frac{1}{L}\left(\eta\frac{dL}{dt} + q_{lm} - \int_0^{L\eta} N d\eta\right)\frac{\partial \epsilon_s}{\partial \eta} - (1-\epsilon_s)N = \frac{1}{L^2}\frac{\partial}{\partial \eta}\left[\frac{k^0 p_A}{\mu\beta}\left(\frac{\epsilon_s}{\epsilon_s^0}\right)^{(1-\delta)/\beta}(1+\alpha_1\epsilon_{s2}^{\alpha_2})^{-1}\frac{\partial \epsilon_s}{\partial \eta}\right] \tag{53}$$

$$\frac{\partial \epsilon_{s2}}{\partial t} - \frac{1}{L}\left(\eta\frac{dL}{dt} + q_{lm}\cdot\int_0^{L\eta} N d\eta\right)\frac{\partial \epsilon_{s2}}{\partial \eta} - (1-\epsilon_{s2})N$$
$$= \frac{1}{L^2}\frac{\partial}{\partial \eta}\left[\frac{k^0 p_A}{\mu\beta}\left(\frac{\epsilon_s}{\epsilon_s^0}\right)^{(1-\delta)/\beta}\epsilon_s^{-1}\epsilon_{s2}(1+\alpha_1\epsilon_{s2}^{\alpha_2})^{-1}\frac{\partial \epsilon_s}{\partial \eta}\right] \quad (54)$$

$$-n_2\frac{\partial \epsilon_s}{\partial t} + (1-\epsilon_s)\frac{\partial n_2}{\partial t} - \frac{1}{L}\left(\eta\frac{dL}{dt} + q_{lm}\cdot\int_0^{L\eta} N d\eta\right)$$
$$\times\left[(1-\epsilon_s)\frac{\partial n_2}{\partial \eta} - n_2\frac{\partial \epsilon_s}{\partial \eta}\right] + [1+n_2(1-\epsilon_s)]N$$
$$= -\frac{1}{L^2}\frac{\partial}{\partial \eta}\left[\frac{k^0 p_A}{\mu\beta}\left(\frac{\epsilon_s}{\epsilon_s^0}\right)^{(1-\delta)/\beta} n_2(1+\alpha_1\epsilon_s^{\alpha_2})^{-1}\frac{\partial \epsilon_s}{\partial \eta}\right] \quad (55)$$

Comparing above expressions with Eq. 53, P_{ij}, Q_i and R_i are found to be

$$P_{11}=1, \quad P_{12}=0, \quad P_{13}=0 \quad (56)$$
$$P_{21}=0, \quad P_{22}=1, \quad P_{23}=0 \quad (57)$$
$$P_{31}=-n_2, \quad P_{32}=0, \quad P_{33}=1-\epsilon_s \quad (58)$$
$$Q_1 = -\frac{1}{L}\left(\eta\frac{dL}{dt} + q_{lm}\cdot\int_0^{L\eta} N d\eta\right)\frac{\partial \epsilon_s}{\partial \eta} - (1-\epsilon_s)N \quad (59)$$
$$Q_2 = -\frac{1}{L}\left(\eta\frac{dL}{dt} + q_{lm}\cdot\int_0^{L\eta} N d\eta\right)\frac{\partial \epsilon_{s2}}{\partial \eta} - (1-\epsilon_{s2})N \quad (60)$$
$$Q_3 = -\frac{1}{L}\left(\eta\frac{dL}{dt} + q_{lm}\cdot\int_0^{L\eta} N d\eta\right)\left[(1-\epsilon_s)\frac{\partial n_2}{\partial \eta} - n_2\frac{\partial \epsilon_s}{\partial \eta}\right] + [1+n_2(1-\epsilon_s)]N \quad (61)$$
$$R_1 = \frac{1}{L^2}\frac{k^0 p_A}{\mu\beta}\left(\frac{\epsilon_s}{\epsilon_s^0}\right)^{(1-\delta)/\beta}(1+\alpha_1\epsilon_{s2}^{\alpha_2})^{-1}\frac{\partial \epsilon_s}{\partial \eta} \quad (62)$$
$$R_2 = \frac{1}{L^2}\frac{k^0 p_A}{\mu\beta}\left(\frac{\epsilon_s}{\epsilon_s^0}\right)^{(1-\delta)/\beta}\epsilon_s^{-1}\epsilon_{s2}(1+\alpha_1\epsilon_{s2}^{\alpha_2})^{-1}\frac{\partial \epsilon_s}{\partial \eta} \quad (63)$$
$$R_3 = -\frac{1}{L^2}\frac{k^0 p_A}{\mu\beta}\left(\frac{\epsilon_s}{\epsilon_s^0}\right)^{(1-\delta)/\beta} n_2(1+\alpha_1\epsilon_s^{\alpha_2})^{-1}\frac{\partial \epsilon_s}{\partial \eta} \quad (64)$$

Boundary conditions

(a) *Constant Rate Filtration.* To meet the format of Eq. 50, Eq. 26 is rewritten as

$$q_{lm} = -\frac{1}{L}\frac{k^0 p_A}{\mu\beta}\left(\frac{\epsilon_s}{\epsilon_s^0}\right)^{(1-\delta)/\beta}\epsilon_s^{-1}(1+\alpha_1\epsilon_{s2}^{\alpha_2})^{-1}\frac{\partial \epsilon_s}{\partial \eta} \quad (65)$$

According to Eq. 50 and Eq. 62, the boundary conditions of Eq. 53 are

$$\text{at } \eta=0, \quad \beta_1=1 \quad \gamma_1 = -q_{lm}\cdot\epsilon_s/L \quad (66a)$$
$$\eta=1, \quad \beta_1=0 \quad \gamma_1 = \epsilon_s - \epsilon_s^0 \quad (66b)$$

For Eq. 54, it is assumed that there is no retention of type 2 particles at the cake-slurry interface ($\eta = 0$). Thus, the boundary conditions of Eq. 54 are

$$\text{at } \eta=0, \quad \beta_2=1 \quad \gamma_2 = -q_{lm}\cdot\epsilon_{s2}/L \quad (67a)$$
$$\eta=1, \quad \beta_2=0 \quad \gamma_2 = \epsilon_{s2} \quad (67b)$$

For the boundary conditions of Eq. 55, the concentration of type 2 particles n_2 at the cake-slurry interface can be assumed to be n_2^0, i.e., the concentration of d_{p2} in the slurry. To derive the boundary condition at the cake-media interface, one may apply the general rate equation in deep bed filtration to the present case, or

$$\frac{\partial n_2}{\partial \eta} = \lambda n_2 \quad (68)$$

Integrating the above equation, one has

$$n_2 = (n_2)_{\eta=0} = n_2^0 \exp\left(-L\int_0^1 \lambda d\eta\right) \quad (69)$$

Therefore, the boundary conditions of Eq. 55 are

$$\text{at } \eta=0, \quad \beta_3=0 \quad \gamma_3 = n_2 - (n_2)_{\eta=0} \quad (70a)$$
$$\eta=1, \quad \beta_3=0 \quad \gamma_3 = n_2 - n_2^0 \quad (70b)$$

(b) *Constant Pressure Filtration.* The boundary conditions for the constant pressure case are the same as those of the constant rate case, except that q_{lm} is now given by Eq. 26.

The following expression is used for the local filter coefficient of Type 2 particles

$$\lambda = \lambda_0\left(1+\frac{\beta'\epsilon_{s2}}{1-\epsilon_s}\right)\left(1-\frac{\epsilon_{s2}}{1-\epsilon_s}\right) \quad (71)$$

where λ_0 is the initial value of λ (i.e., when there is no retained type 2 particles) and β' is an empirical constant. As an empirical expression, Eq. 68 has been found applicable in representing filter coefficient data (see Tien, 1989).

Initialization of the numerical solution

To initiate the numerical solution, the following procedure may be used.

For time up to t_0, t_0 is an arbitrarily small value, the cake formed may be considered to be incompressible. Consequently, one may assume that $q_s = 0$. Equation 18 becomes

$$N = \left|q_l - q_s\frac{1-\epsilon_s}{\epsilon_s}\right|\lambda n_2 = q_l\lambda n_2 \quad (72)$$

During the period $0 < t < t_0$, ϵ_{s2} may be assumed negligible. From Eq. 71, λ may be approximated to be λ_0. Integrating Eq. 68 from $x = x$ to $x = L$ yields

$$n_2 = n_2^0 e^{-\lambda_0(L-x)} \quad (73)$$

The rate of filtration, during this interval, can be found from Eqs. 73 and 72, or

$$N = |q_l|\lambda_0 n_2^0 e^{-\lambda_0(L-x)} \tag{74}$$

If the cake is incompressible, $q_s = 0$. From Eq. 16, one has

$$\frac{\partial q_l}{\partial x} = N = q_l \lambda_0 n_2^0 e^{-\lambda_0(L-x)} \tag{75}$$

The integrated form of Eq. 75 is

$$q_l = q_{lm} e^{-n_2^0 e^{-\lambda_0 L}(e^{\lambda_0 x}-1)} \tag{76}$$

The rate of filtration N is therefore

$$N = q_{lm} e^{-n_2^0 e^{-\lambda_0 L}(e^{\lambda_0 x}-1)} \lambda_0 n_2^0 e^{-\lambda_0(L-x)} \tag{77}$$

The integrated form of Eq. 16 is

$$q_l = q_{lm} + \int_0^x N dx \tag{78}$$

From Eqs. 78 and 21, one has

$$q_l = \frac{k}{\mu}\frac{\partial p_s}{\partial x} \tag{79}$$

Combining Eqs. 79 and 76 yields

$$\frac{k}{\mu}\frac{\partial p_s}{\partial x} = q_{lm} e^{-n_2^0 e^{-\lambda_0 L}(e^{\lambda_0 x}-1)} \tag{80}$$

To obtain the profile of p_s, one may rewrite Eq. 80 as

$$\frac{k}{\mu}\frac{\partial p_s}{\partial x} = q_{lm} f(x) \tag{81}$$

where

$$f(x) = e^{-n_2^0 e^{-\lambda_0 L}(e^{\lambda_0 x}-1)} \tag{82}$$

Since the cake thickness is thin, $f(x)$ may be approximated by Taylor series as

$$f(x) = 1 - n_2^0 \lambda_0 e^{-\lambda_0 L} x \tag{83}$$

Substituting Eqs. 28 and 83 into Eq. 81 and noting $\epsilon_{s2} \approx 0$, one has

$$\frac{k_0}{\mu}\left(1+\frac{p_s}{p_A}\right)^{-\delta}\frac{\partial p_s}{\partial x} = q_{lm}(1 - n_2^0 \lambda_0 e^{-\lambda_0 L})x \tag{84}$$

Integrating the above expression across the cake yields

$$\frac{k_0}{\mu} p_A \frac{\left[1-\left(1+\frac{p_{sm}}{p_A}\right)^{1-\delta}\right]}{1-\delta} = q_{lm}\left(L - \frac{1}{2} n_2^0 \lambda_0 e^{-\lambda_0 L} L^2\right) \tag{85}$$

where p_{sm} is the value of p_s at $x = 0$ (i.e., medium surface). Equation 85 gives the relationship between L and p_{sm}.

Also for small time, with cake being incompressible, namely $\epsilon_s = \epsilon_s^0 =$ constant and negligible retention, the cake thickness for the constant pressure and constant rate cases are

$$L = \frac{c^0 t_0}{\epsilon_s^0 - c^0}\frac{Rk^0}{\mu}(p_0 - p_{sm}) \quad \text{for constant pressure filtration} \tag{86a}$$

$$L = \frac{c^0 t_0}{\epsilon_s^0 - c^0} q_{lm} \quad \text{for constant rate filtration} \tag{86b}$$

The compressive stress profile across the cake can be found from the integration of Eq. 84 [from $x = x$ to $x = L$] together with Eq. 85 as

$$\left(1+\frac{p_s}{p_A}\right)^{1-\delta} = \left(1+\frac{p_{sm}}{p_A}\right)^{1-\delta} - \left[\left(1+\frac{p_{sm}}{p_A}\right)^{1-\delta} - 1\right]\eta \tag{87}$$

To initiate the numerical solution, the values of L and p_{sm} are found from the solutions of Eqs. 85 and 86. Once p_{sm} is known, the values of p_s as a function of η can be found from Eq. 87. The corresponding values of ϵ_s can be determined from the constitutive equation of Eq. 24 once the values of p_s are known. n_2 can be found from Eq. 73 while ϵ_s is assumed to be negligible.

Computer Programs

Fortran programs calling D03PCF to solve the set of equations for cake filtration were written. The programs first calculated the initial profiles of ϵ_s, ϵ_{s2}, n_2, p_s and the value of L at t_0. Subroutine D03PCF was then called to solve the system of PDEs for the new profiles of ϵ_s, ϵ_{s2}, n_2 and p_s at t_1 ($t_1 = t_0 + \Delta t$). The cake thickness L at t_1 was determined as

$$L_{t_1} = \frac{c^0}{(U1)_{t_1} - (U2)_{t_1} - c^0}\sum_{t=t_0}^{t=t_1} q_{lm}\Delta t \tag{88}$$

where c^0 is the solid fraction of particles of d_{p1} in the slurry, and $(U1)_{t1}$ and $(U2)_{t1}$ are given as

$$(U1)_{t_1} = \int_0^1 (\epsilon_s)_{t_1} d\eta \tag{89}$$

$$(U2)_{t_1} = \int_0^1 (\epsilon_{s2})_{t_1} d\eta \tag{90}$$

The cake growth rate dL/dt at t_1 was calculated from Eq. 47, i.e.

$$\left(\frac{dL}{dt}\right)_{t_1} = \frac{\epsilon_s^0}{\epsilon_s^0 - c^0}\left[\left(\frac{k}{\mu}\frac{\partial p}{\partial x}\right)_{L^-}\right]_{t_1} - \left[\left(\frac{k}{\mu}\frac{\partial p}{\partial x}\right)_0\right]_{t_1} + \left[\int_0^L N dx\right]_{t_1} \quad (91)$$

The spatial derivative $(\partial p/\partial x)_{L^-}$ at t_1 in Eq. 91 was approximated by a five-point backward finite difference approximation as

$$\left(\frac{\partial p}{\partial x}\right)_{L^-} = -\frac{1}{12\Delta x}[3p_s(m-4) - 16p_s(m-3) + 36p_s(m-2) - 48p_s(m-1) + 25p_s(m)] \quad (92)$$

where m is the number of mesh points in the spatial direction, $\Delta x = L/m$ is the corresponding spatial interval, and $p_s(m)$ denotes the compressive stress at the cake-slurry interface at t_1.

To calculate the third term on the righthand side of Eq. 91 at t_1, from Eqs. 18 and 19a

$$N = \frac{k}{\mu}\frac{\partial p}{\partial x}\lambda n_2 = -\frac{1}{L}\frac{k}{\mu}\frac{\partial p_s}{\partial \eta}\lambda n_2 \quad (93)$$

At each mesh point j ($j = 0, 1, \ldots\ldots, m$) at time t_1, $\partial p_s/\partial \eta$ was evaluated by the two-point forward finite difference approximation (for $j = 0$), or the two-point backward finite difference approximation (for $j = m$) or the three-point central finite difference approximation (for $j \neq 0$ and m). Then the values of N_j ($j = 0, 1, \ldots\ldots, m$) at time t_1 was calculated according to Eq. 93 (noting that λ is defined by Eq. 71). Finally, the Simpson integration rule was used to obtain the value of integral, $\int_0^L N dx$, which, in turn, gave the value of dL/dt.

With the profiles of ϵ_s, ϵ_{s2}, n_2, p_s and the values of L and dL/dt known at t_1, subroutine D03PCF was once again called to give the new profiles of ϵ_s, ϵ_{s2}, n_2 and p_s at t_2. Then the same procedure above was followed to obtain the values of L and dL/dt at t_2. This procedure was repeated until the final time t specified in the numerical calculation was reached.

Sample Calculation Results

A number of sample calculations were made under both constant-rate and constant pressure modes of operation. The sample calculation results include cake thickness L, filtration rate q_{lm} and filtrate volume (for the constant-pressure case) and applied pressure p_0 (for the constant-rate case) as functions of time as well as the profiles of ϵ_s, ϵ_{s2}, p_s, n_2 and k at various times. The values of the parameters used in the sample calculations are listed in Table 1. The sample calculation results are summarized as follows:

Table 1. Parameters and their Values Used in Sample Calculation

ϵ_s^0	0.269	c^0	0.20
δ	0.49	t_0	0.1 s
β	0.09	R	100 (m^{-1})
p_a	1,200 (Pa)	β'	5.0
k^0	3.4965×10^{-15} (m^2)	α_1	30.0
μ	0.001 (Pa·s)	α_2	1.0
p_0 (const. pres.)	900,000 (Pa)	n_{20}	0.05, 0.01, 0.0005
q_{lm} (const. rate)	2.0×10^{-5} ($m^3/s \cdot m^2$)	λ_0	0, 10, 100

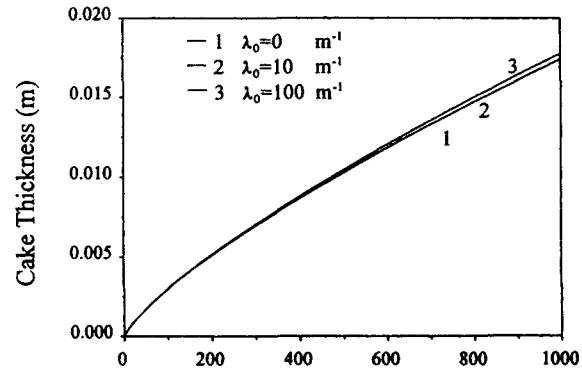

Figure 2. Predicted cake thickness vs. time.

Constant rate filtration with $n_2^0 = 0.05$ and three different values of λ_0.

Constant Rate Case. The results are shown from Figures 2 to 8. Figure 2 shows the increase of cake thickness as a function of time for three different values of λ_0. For a suspension with low fine particle concentration (500 ppm), fine particle retention does not significantly change the cake thickness although a slight increase in cake thickness at high retention rate was observed. Figure 3 gives the total solidosity profile within the cake at different times. It can be seen that retention of fine particles may contribute substantially to ϵ_s, especially at larger filtration times (say $t = 1{,}000$ s). Figure 4 depicts the distribution of the deposited type 2 particles within the cake. Great differences in the values of ϵ_{s2} are seen as the value of λ_0 increases from 10 to 100 m^{-1}. At small value of t, the steepness of the ϵ_{s2} profile is more pronounced at the lower level of the cake (i.e., small value of x/L). The profile was found to approach an S shaped curve at $t = 1{,}000$ s; indicating a slowdown of the accumulation of deposited fine particles near the septum because of the reduction of fine particles in the suspension flowing through the cake. In Figure 5, the profiles of fine particle concentrations of the

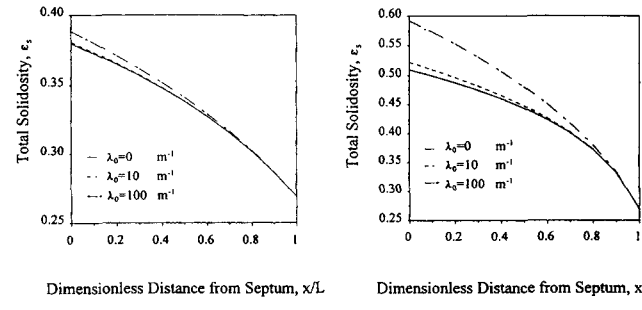

Figure 3. Predicted total solidosity profiles across the cake.

Constant rate filtration with $n_2^0 = 0.05$ and three different values of λ_0.

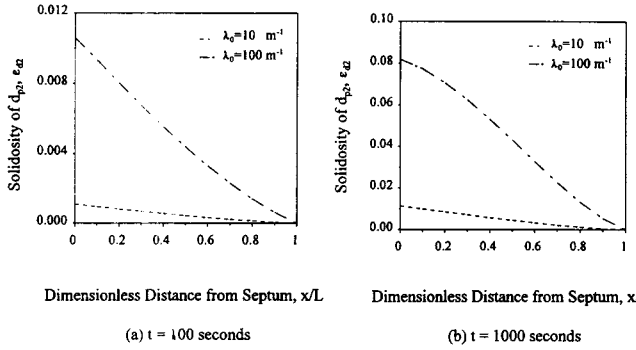

Figure 4. Predicted profiles of deposited fine particles across a cake.

Constant rate filtration with $n_2^0 = 0.05$ and two different values of λ_0.

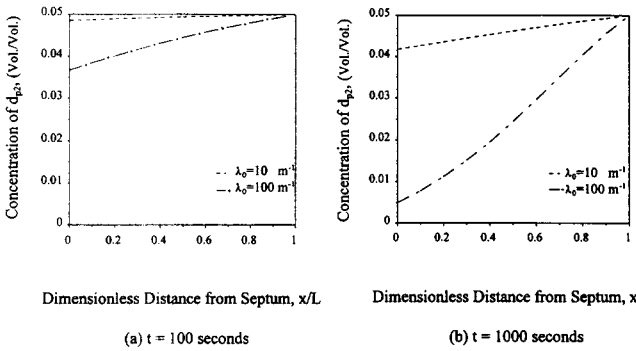

Figure 5. Predicted fine particle concentrations of the suspension flowing through a cake.

Constant rate filtration with $n_2^0 = 0.05$ and two different values of λ_0.

suspension flowing through the cake are shown. With the increase of t, the fine particle concentration profile exhibits a more rapid decline near the septum and then levels off. This is consistent with the results shown in the preceding figure. As shown before, greater fine particle retention results in a denser cake and therefore a higher value of the compressive stress. The trend of p_s is also shown in Figure 6. At $x = 0$ and $t = 1{,}000$ s, for example, the value of p_s for the case of $\lambda_0 = 100$ m^{-1} is four times the value of that of $\lambda_0 = 0$ (i.e., no

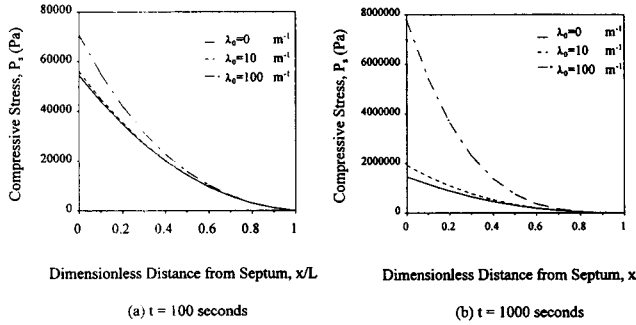

Figure 6. Predicted compressive stress profiles within a cake.

Constant rate filtration with $n_2^0 = 0.05$ and three different values of λ_0.

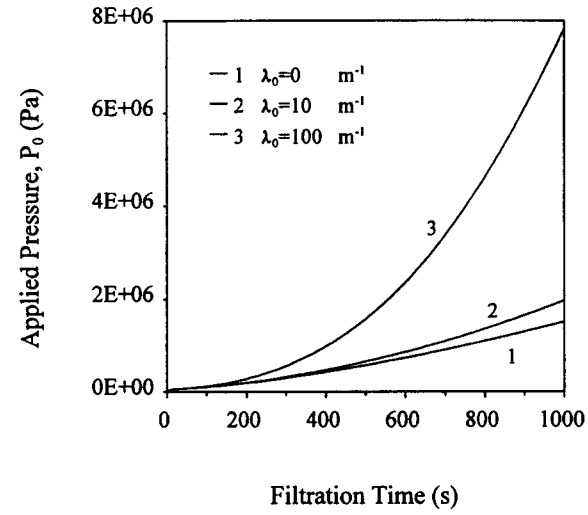

Figure 7. Predicted pressure requirement vs. time.

Constant rate filtration with $n_2^0 = 0.05$ and three different values of λ_0.

fine particle retention). The increase in compressive stress arises directly from the rapid increase in p_0 necessary to maintain a constant rate filtration operation as shown in Figure 7. The corresponding permeability profiles are given in Figure 8.

Constant Pressure Case. The sample calculation results of this case are shown in Figures 9 to 15. The deposited fine particle profiles and suspended fine particle profiles across the cake (Figures 9 and 10, respectively) are similar to those of the constant rate case.

Figure 11 gives the predicted cake thickness vs. time. It shows that the cake thickness will be lower at a higher value of λ_0. In constant pressure filtration, fine particle retention leads to a significant reduction in filtrate flux, which, in turn, decreases the cake thickness. The predicted filtration rate vs. time and the total filtrate volume vs. time are shown in Figures 12 and 13. The effect of fine particle retention on filtration performance is clearly indicated in these two figures. In the constant pressure case, the total ϵ_s profile displays a behavior different from that observed in the constant rate case. As shown in Figure 14, ϵ_s remains relatively constant near the cake-septum interface ($x = 0$) for different values of λ_0.

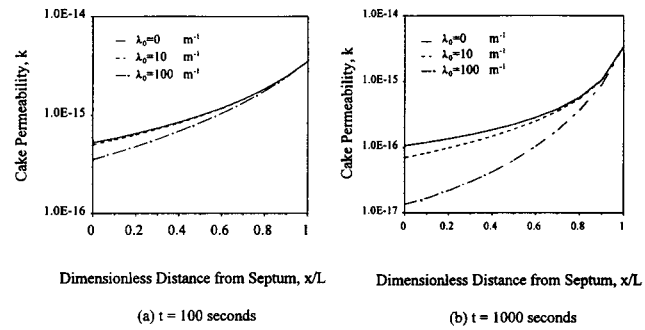

Figure 8. Predicted profiles of cake permeability in a cake.

Constant rate filtration with $n_2^0 = 0.05$ and three different values of λ_0.

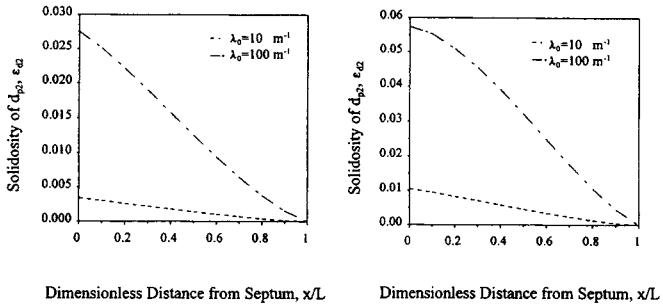

Figure 9. Predicted deposited fine particle concentration profiles across a cake.

Constant pressure filtration with $n_2^0 = 0.05$ and two different values of λ_0.

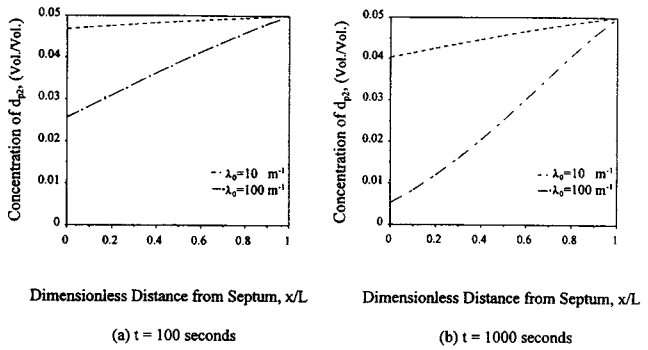

Figure 10. Predicted fine particle concentrations of the suspension flowing through a cake.

Constant pressure filtration with $n_2^0 = 0.05$ and two different values of λ_0.

Within the cake, however, a lower value of ϵ_s was predicted for a higher λ_0 value. The compressive stress profiles, which are given in Figure 15, display the same trend as that of the total solidosity profiles of Figure 14.

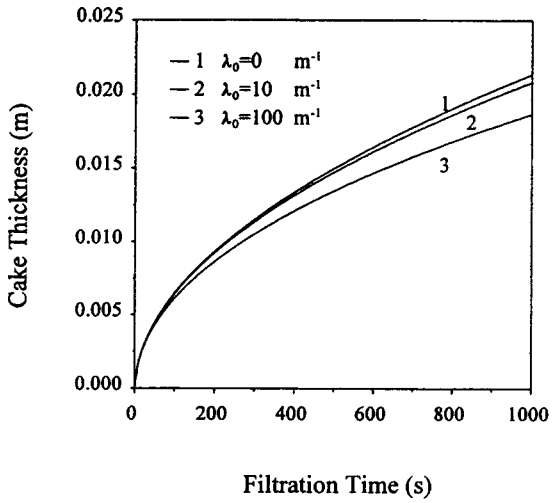

Figure 11. Predicted cake thickness vs. time.

Constant pressure filtration with $n_2^0 = 0.05$ and three different values of λ_0.

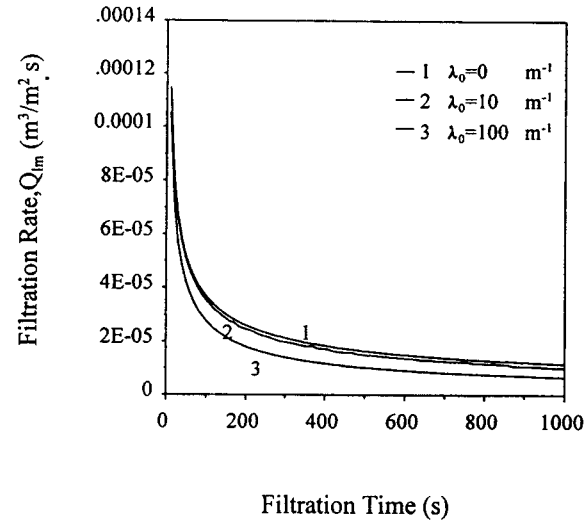

Figure 12. Predicted filtration rate vs. time.

Constant pressure filtration with $n_2^0 = 0.05$ and three different values of λ_0.

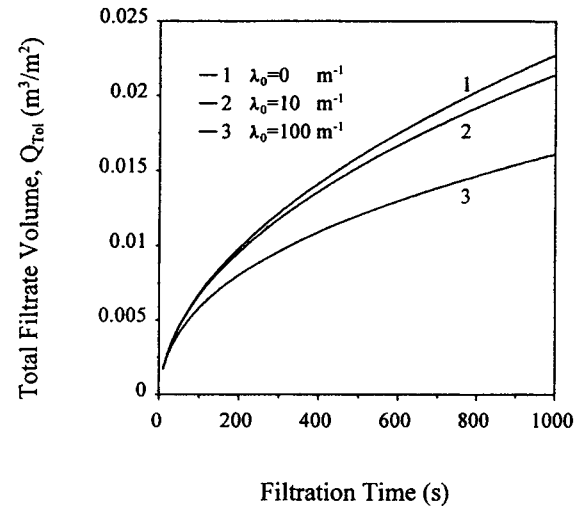

Figure 13. Total filtration volume vs. time.

Constant pressure filtration with $n_2^0 = 0.05$ and three different values of λ_0.

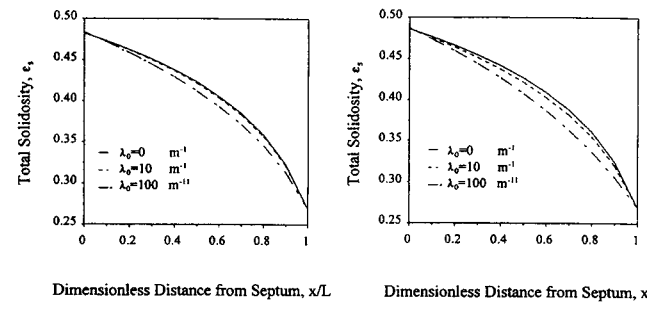

Figure 14. Predicted total solidosity profiles across a cake.

Constant pressure filtration with $n_2^0 = 0.05$ and three different values of λ_0.

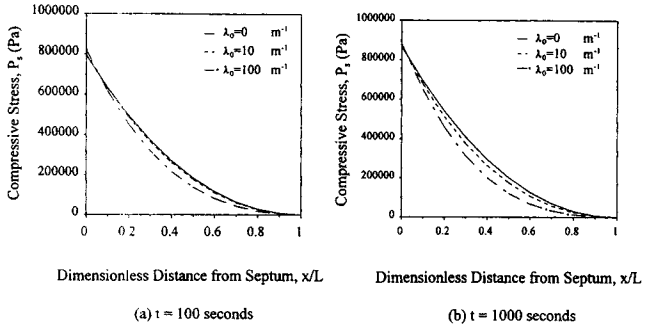

Figure 15. Predicted compressive stress profiles across a cake.

Constant pressure filtration with $n_2^0 = 0.05$ and three different values of λ_0.

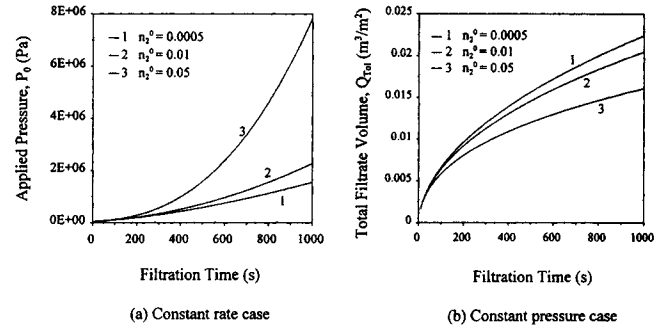

Figure 17. Comparison of filtration performance at different values of n_2^0 with $\lambda_0 = 100$ m^{-1}.

An interesting issue concerning fine particle retention is the significance of the permeability change induced due to cake clogging. From Eq. 28, it can be seen that the scaled local permeability function (k/k^0) is the product of two factors. The first represents the compression effect and the second term accounts for the effect of fine particle retention. The relative importance of these two factors is shown in Figure 16 in which the quantities $(1 + p_s/p_A)^{-\delta}]$ and $(1 + \alpha_1 \epsilon^{\alpha 2})^{-1}]$, across the cake at different times are shown.

Effect of Fine Particle Concentration. The results presented above are those of a suspension with $n_2^0 = 0.05$. As expected, a change of the fine particle concentration impacts significantly on filtration performance. As an indication, Figure 17 gives the pressure required vs. time of the constant rate case and the filtrate volume vs. time of the constant pressure case with different volumes of n_2^0. When the values of n_2^0 were increased from 0.0005 to 0.05, the pressure required of the constant rate case significantly increased. Similarly, the filtrate volume of the constant pressure case is greatly reduced. It is easy to understand that with higher volume of n_2^0, more fine particles will be retained in the cake, hence the observed behaviors.

Evaluation of Constitutive Relationships from Filtration /Data

We present in the following results on the determination of constitutive relationships from filtration data to further demonstrate the effect of fine particle retention. The relationship between ϵ_s and p_s is given by Eq. 27. In the absence of fine particle retention, the relationship between k and p_s given by Eq. 28 reduces to

$$k = k^0 \left(1 + \frac{p_s}{p_A}\right)^{-\delta} \tag{94}$$

Assuming that Eqs. 27 and 94 are valid over limited ranges of p_s for all systems, determining constitutive relationships from experimental data means the estimation of the values of ϵ_s^0, p_A, β, k^0 and δ which best fit the data.

Similar to any parameter search problem, one may define an objective function Φ to be

$$\Phi = \sum_{i=1}^{m'} \left[(A)^E_j - (A)^P_j\right]^2 \tag{95}$$

where A is a measurable quantity of cake filtration (A may be taken to be the pressure required for constant rate filtration and the filtrate volume for constant pressure filtration). The superscripts E and P denote respectively the experimental and predicted values. The subscript, j, refers to the jth measurement and there are m' data points. Parameter search is carried out by the minimization of the object function.

The parameter search results are given in Table 2. The parameter search results shown in the first part of Table 2 were based on the results shown in Figure 7. The three curves of Figure 7 give the required pressure vs. time for constant rate filtration under the conditions specified in Table 1 for three cases: no particle retention, moderate particle reten-

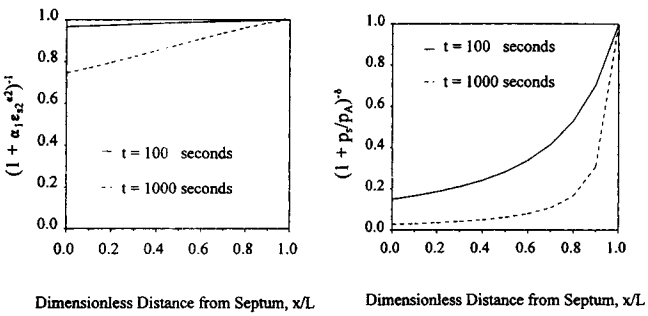

Figure 16. Effect of the factors $(1+\alpha_1\epsilon_{s2}{}^{\alpha 2})^{-1}$ and $(1+p_s/p_A)^{-\delta}$ in Eq. 28 on the permeability of k in the cake ($\lambda_0 = 10$, $\alpha_1 = 30$, $\alpha_2 = 1$, $\delta = 0.49$, $p_A = 1{,}200$).

Table 2. Parameters in Constitutive Relationships Based on Test Data

Filtration Mode		p_A	β	δ	ϵ_s^0	k^0
Constant Rate	$\lambda_0 = 0$	1,200	0.4900	0.0900	0.269	3.5^{15}
	$\lambda_0 = 10$ m^{-1}	2,942.6	0.6010	0.0902	0.2913	3.5^{15}
	$\lambda_0 = 100$ m^{-1}	2,780.1	0.6978	0.0900	0.290	3.5^{15}
Constant Pressure	$\lambda_0 = 0$	1,200	0.4900	0.0900	0.269	3.5^{15}
	$\lambda_0 = 10$ m^{-1}	1,188.1	0.5242	0.0900	0.269	3.5^{15}
	$\lambda_0 = 100$ m^{-1}	1,925	0.6746	0.0926	0.2779	3.5^{15}

tion, and heavy particle retention. For the case of no fine particle retention, the searched results were nearly identical to those used for simulating the results (there is a small difference for k^0). On the other hand, if the two other cases of data shown in Figure 7 were used as the basis of parameter search and assuming that there was no fine particle retention, the parameter values obtained were significantly different from the correct values (see values along the third and fourth rows of Table 2). The difference is understandable since the various parameter values must be adjusted to account for the decrease in permeability due to cake clogging because of fine particle retention.

The results for the constant pressure case are similar. For the parameter search of the constant pressure cases, the results shown in Figure 13 were used. For this case, based on the results of q_{lm} vs. time with no fine particle retention, the parameter search yields results which were nearly identical to those used for generating results. The parameter values obtained were found to deviate from the correct values with slight fine particle retention and deviate significantly if the extent of fine particle was great.

Conclusion

A rigorous analysis of cake filtration based on the multiphase flow theory, Darcy's law, and the constitutive equation relating the state of the cake with the compressive stress was presented. The analysis considers the effects of fine particle retention within a cake while the cake is being formed. The fine particle retention effect was analyzed as a deep-bed filtration problem with the filter coefficient considered as a constant.

It is shown that the reduction in local permeability of a filter cake results from two factors: cake consolidation and cake clogging. Cake consolidation arises from the compressive stress within the cake while cake clogging is caused by the retention of fine particle. The amount of the fines involved may be small; its effect on permeability, however, can be substantial. The importance of considering the fine particle retention effect in determining the constitutive relationships from test filter data was demonstrated in a sample calculation.

Acknowledgment

This study was performed under the Solid/Liquid Separation grant, National Science and Technology Board, Republic of Singapore.

Literature Cited

Chase, G. G., "Continuum Analysis of Constant Rate Cake Filtration," PhD Diss., Univ. of Akron, Akron, OH (1989).

Ruth, B. F., G. H. Montillon, and R. E. Montonna, "Studies in Filtration: I. Critical Analysis of Filtration Theory; II. Fundamentals of Constant Pressure Filtration," *Ind. Eng. Chem.*, **25**, 76, 153 (1933).

Shirato, M., M. Sambuichi, H. Kato, and T. Aragaki, "Internal Flow Mechanism in Filter Cakes," *AIChE J.*, **15**, 405 (1969).

Shirato, M., T. Murase, E. Ivitari, F. M. Tiller, and A. F. Alciatore, "Filtration in the Chemical Process Industry," in *Filtration: Principle and Practice*, M. J. Matteson and C. Orr, eds., 2nd ed., Marcel Dekker, New York (1987).

Stamatakis, K., and C. Tien, "Cake Formation and Growth in Cake Filtration," *Chem. Eng. Sci.*, **46**, 1917 (1991).

Tien, C., *Grandular Filtration of Aerosols and Hydrosols*, Butterworths, Stoneham, MA (1989).

Tiller, F. M., and C. S. Yeh, "Introduction to Solid-Liquid Separation Principles and Theoretical Aspects," *Adv. Solid-Liquid Separation*, H. Muralidhara, ed., Roy. Soc. of Chemistry, London (1986).

Tiller, F. M., and H. R. Cooper, "The Role of Porosity in Filtration: IV. Constant Pressure Filtration," *AIChE J.*, **6**, 595 (1960).

Tiller, F. M., and J. R. Crump, "Recent Advances in Compressible Cake Filtration Theory," in *Mathematical Models and Design Methods in Solid-liquid Separation*, A. Rushton, ed., Martinus Nijhoff, Dordrecht (1985).

Tiller, F. M., and M. Shirato, "The Role of Porosity in Filtration: VI. New Definition of Filtration Resistance," *AIChE J.*, **10**, 61 (1964).

Wakeman, R. J., "A Numerical Solution of the Differential Equations Describing the Formation of Air Flow in Compressible Filter Cakes," *Trans. Instn. Chem. Engrs.*, **56**, 258 (1978).

Willis, M. S., I. Tosun, W. Choo, G. G. Chase, and F. Desai, "Dispersed Multiphase Theory and its Application to Filtration," *Adv. in Porous Media*, M. Y. Corapcioglu, ed., Elsevier, New York (1991).

Manuscript received Mar. 14, 1996, and revision received July 12, 1996.